NeuroImage 43 (2008) 410–419

Contents lists available at ScienceDirect

NeuroImage

journal homepage: www.elsevier.com/locate/ynimg

Phase-locking within human mediotemporal lobe predicts memory formation

Juergen Fell [a,*], Eva Ludowig [a], Timm Rosburg [a], Nikolai Axmacher [a,b], Christian E. Elger [a,b]

[a] Department of Epileptology, University of Bonn, Sigmund-Freud Str. 25, D-53105 Bonn, Germany
[b] Life and Brain Center of Academic Research, Sigmund-Freud-Str. 25, 53127 Bonn, Germany

ARTICLE INFO

Article history:
Received 21 February 2008
Revised 19 June 2008
Accepted 7 July 2008
Available online 22 July 2008

Keywords:
Memory
Rhinal cortex
Hippocampus
Intracranial EEG
Phase-locking

ABSTRACT

Lesion and imaging studies have demonstrated that encoding of declarative memories, i.e. consciously accessible events and facts, is supported by processes within the rhinal cortex and the hippocampus, two substructures of the mediotemporal lobe (MTL). Successful memory formation has, for instance, been shown to be accompanied by the rhinal N400 component, followed by a hippocampal positivity, as well as by transient rhinal–hippocampal phase synchronization. However, it has been an open question, which mediotemporal electroencephalogram (EEG) measures predict memory formation most accurately. Therefore, we analyzed and compared the association of different mediotemporal EEG measures with successful memory formation. EEG characteristics were extracted from intracranial rhinal and hippocampal depth recordings in 31 epilepsy patients performing a continuous word recognition paradigm. Classical event-related potential measures, rhinal–hippocampal synchronization, as well as inter-trial phase-locking and power changes within rhinal cortex and hippocampus were evaluated. We found that inter-trial phase-locking is superior to other EEG measures in predicting subsequent memory. This means that memory formation is related to the precise timing of EEG phases within the MTL with respect to stimulus onset. In particular, early rhinal and hippocampal phase-locking in the alpha/beta range reaching its maximum already between 100 and 300 ms after stimulus onset appears to be a precursor of successful memory formation. Our data suggest that early mediotemporal phase adjustments constitute a relevant mechanism underlying declarative memory encoding.

Introduction

Lesion and imaging studies have demonstrated that encoding of declarative memories, i.e. consciously accessible events and facts, depends on processes within the rhinal cortex and the hippocampus, two substructures of the mediotemporal lobe (MTL) (e.g. Eichenbaum, 2000; Squire et al., 2004). Successful memory formation has, for instance, been shown to be associated with different mediotemporal event-related potential (ERP) components and electroencephalogram (EEG) measures: the rhinal N400 component and a later hippocampal positivity (Grunwald et al., 1999; Fernández et al., 1999, 2002), rhinal–hippocampal phase synchronization in the gamma and low frequency range (Fell et al., 2001; 2003), rhinal and hippocampal inter-trial phase-locking (Mormann et al., 2005), as well as an increase of hippocampal power in the upper gamma range and a decrease mainly in the alpha and beta range (Sederberg et al., 2007). All these measures carry different information. Phase synchronization characterizes the coupling between two brain regions as given by the variability of phase differences across trials. Inter-trial phase-locking specifies the phase stability at a certain brain region, i.e. how temporally precise the phase of an EEG response is locked to stimulus onset. Phase-locking and power changes are complementary aspects, which differentially contribute to averaged ERPs depending on the cognitive task (e.g. Fell et al., 2004; Klimesch et al., 2004; Makeig et al., 2004; Mazaheri and Jensen, 2006). However, it has been yet an open question, which mediotemporal EEG measures predict memory formation best.

Therefore, we aimed to analyze a variety of EEG measures for the same memory task performed by a large patient group. Intracranial EEG was recorded from 31 patients with pharmacoresistant temporal lobe epilepsies during a continuous word recognition experiment. Data from this experiment are routinely used for the planning of resective surgery. Multicontact depth electrodes had been implanted stereotactically along the longitudinal axis of each MTL (Van Roost et al., 1998) during presurgical evaluation because the seizure onset zone could not be precisely determined with noninvasive investigations. Presurgical evaluation revealed unilateral pathologies for all patients included in the present study. To reduce the possibility of introducing uncontrolled variables brought about by the epileptic process, only those EEG recordings were analyzed that were taken from the MTL contralateral to the zone of seizure origin (Grunwald et al., 1995; Puce et al., 1989). We aimed at comparing both different types (groups) of EEG measures, which possibly correspond to different neural mechanisms, as well as different individual measures with

Abbreviations: EEG, electroencephalogram; MEG, magnetoencephalogram; MTL, mediotemporal lobe; MRI, magnetic resonance imaging.

* Corresponding author. Fax: +49 228 287 16294.
E-mail address: juergen.fell@ukb.uni-bonn.de (J. Fell).

1053-8119/$ – see front matter © 2008 Elsevier Inc. All rights reserved.
doi:10.1016/j.neuroimage.2008.07.021

respect to the ability to predict successful memory formation. For this purpose, we evaluated EEG responses to subsequently remembered and forgotten words by quantifying event-related potential components, frequency band-specific rhinal–hippocampal synchronization, inter-trial phase-locking and power changes. For these groups of measures, EEG characteristics were selected based on a priori hypotheses, if available. In addition, we analyzed characteristics, which showed a strong subsequent memory effect.

Materials and methods

Patients

All patients suffered from pharmacoresistant unilateral temporal lobe epilepsies and were implanted with bilateral depth electrodes along the longitudinal axis of the hippocampus during presurgical evaluation. 31 patients (14 females) with at least one electrode in the rhinal cortex and one electrode in the hippocampus were included in the study. Patients ranged in age from 16 to 61 years (mean 40 years) and in duration of their epilepsy from 4 to 57 years (mean 23 years). At the time of the recordings, all patients received anticonvulsive medication (plasma levels within the therapeutic range). All participants were right-handed and had normal or corrected-to-normal vision. MRI scans or post-surgical histological examinations demonstrated unilateral hippocampal sclerosis in 16 patients (left: 5; right: 11), unilateral extrahippocampal lesions without signs of hippocampal sclerosis in 9 patients (left: 3; right: 6), unilateral hippocampal sclerosis with additional extrahippocampal lesions on the same side in 3 patients (left: 2; right: 1) and no clear lesion in 3 patients. All but two patients underwent subsequent epilepsy surgery after implantation (17 selective amygdalo-hippocampectomies, 7 temporal two-thirds resections, 5 lesionectomies). The word recognition test was conducted as part of the presurgical routine in patients with hippocampal depth electrodes. Informed consent for the intracranial EEG recordings and the use of the data for research purposes was obtained by all patients. The study was approved by the ethics committee of the University of Bonn.

Experimental paradigm

For a continuous word recognition paradigm, 300 frequent German nouns were selected (mean word frequency was 50 per 1 million words according to the CELEX lexical database, version 2.5). 150 stimuli were only presented once, whereas the other 150 words were shown with one repetition. This repetition occurred in 50% of the trials after a short lag of 3 to 6 words and in 50% after a long lag of 10 to 30 words. Thus, 450 words were presented consecutively with a duration of 300 ms per word. The length of the inter-stimulus interval was adjusted to the subjects' abilities (assessed from the responses in a few pilot trials) and was either short (1600±200 ms; n=6), medial (2000±200 ms; n=16) or long (2700±200 ms; n=9). After each word, subjects had to indicate by pressing one of two buttons whether it was new (left button) or already presented before (right button). Subjects used their left and right forefingers for pressing the buttons. The study was conducted in a special unit for simultaneous video- and EEG-monitoring with the patient sitting in an adjustable chair and facing a monitor at a distance of approximately 80 to 100 cm away. The words were presented in white color on a black background with a height of ~1.5° and a width of ~3 to 9° visual angle, depending on word length. Recordings were occasionally repeated with a parallel version of the recognition task on the following day, if performance was bad or ERPs were contaminated by spikes or sharp waves. Performance was considered bad if there was a small amount (<30 correctly recognized “old” or “new” words) of evaluable trials. Throughout, data of the second recordings were used for the analyses in these cases.

EEG recording

Depth electroencephalograms were referenced to linked mastoids, bandpass-filtered (0.01 Hz (6 dB/octave) to 70 Hz (12 dB/octave)), and recorded with a sampling rate of 200 Hz. Electrode contact placement was ascertained by examining MRIs acquired in the sagittal, axial and coronal planes and adjusted to the longitudinal axis of the hippocampus. Electrode contacts were localized based on the individual MRIs and comparison with standardized anatomical atlases (e.g. Duvernoy, 1988; see also Fig. 1). Only EEG recordings from the non-pathological MTL were analyzed. EEG data obtained from the non-pathological MTL in patients with a unilateral seizure origin have been shown to be qualitatively similar to the invasive EEGs recorded in healthy monkeys (Paller et al., 1992). The rhinal electrode was defined as the electrode located within the anterior parahippocampal gyrus (based on the MRI data) with the largest N400 mean amplitude (new words) between 200 and 600 ms (e.g. Grunwald et al., 1999). Because our methods cannot clearly separate perirhinal and entorhinal generators, we use the term rhinal cortex without intending to indicate an integrated rhinal processing stage. The hippocampal electrode was defined as the electrode located within the hippocampus (based on the MRI data) with the largest mean amplitude (new words) of the positive component between 300 and 1500 ms (e.g. Fernández et al., 1999). EEG measures from right and left hemisphere were combined for statistical analyses and figures, because lateralization of verbal memory in MTL epilepsy patients is variable due to functional shifts (e.g. Helmstaedter et al., 2006).

Artifact rejection

An automated artifact rejection was implemented using MATLAB (Mathworks, MATLAB 7.1). For each segment, the standard deviation of the data points as well as the standard deviation of the gradients (the increase or decrease between two successive data points) was determined. A segment was rejected if any data point or gradient deviated more than five standard deviations from the mean. Thus, segments with abnormally high amplitudes as well as abrupt rises or falls were eliminated. For the oscillation analyses, always segments of both electrodes (rhinal and hippocampal) were rejected, if one segment of either position had to be removed. On average, 14% of trials were removed based on these criteria. The data from four patients, which still exhibited artifacts (observed by visual inspection) after applying the automated rejection procedure were discarded from further analysis.

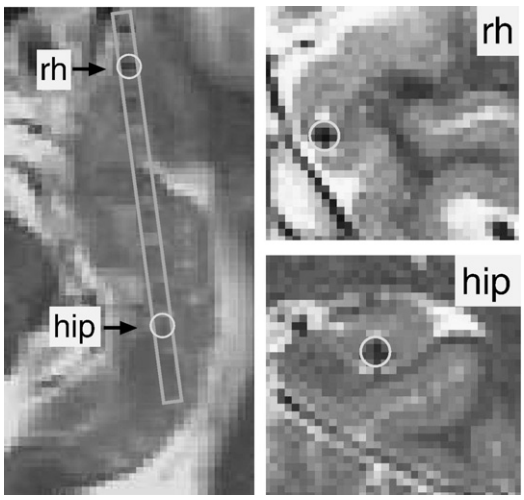

Fig. 1. Exemplary MRI images of one patient showing the selected rhinal (rh) and hippocampal electrode contact (hip) in axial (left) and coronal slices (right).

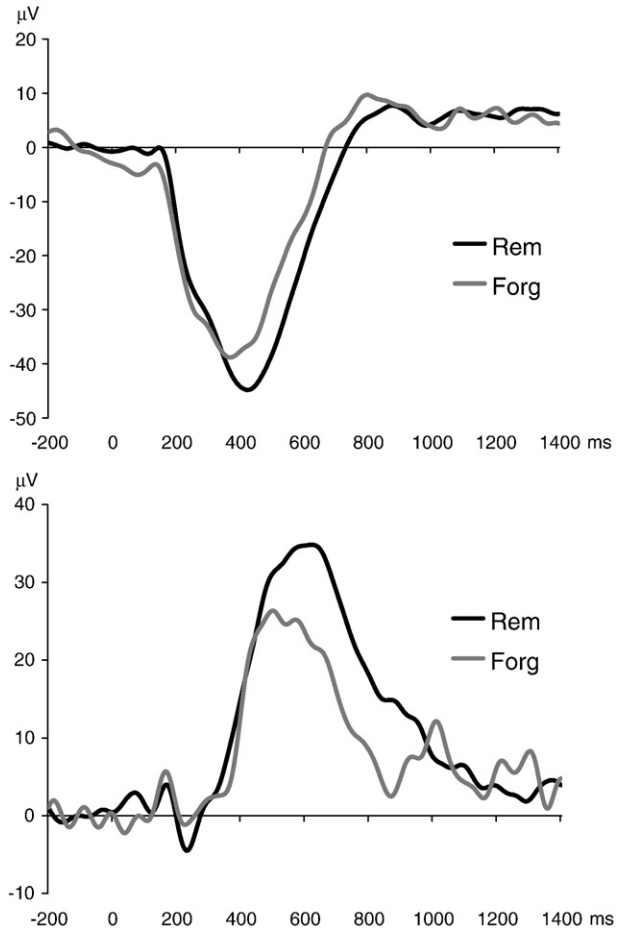

Fig. 2. ERPs after presentation of new words recorded during the continuous recognition experiment. ERPs were averaged separately for a) words that were correctly recognized when presented for the second time (i.e. remembered); b) words that were later not recognized (i.e. forgotten). Above: ERPs recorded from rhinal cortex. Below: ERPs recorded from the hippocampus.

Classical ERP measures

We analyzed the EEG responses to the first presentation of words shown with one repetition. Responses were classified into remembered (REM) or forgotten (FORG) depending on whether the word was subsequently (i.e. at the second presentation) correctly identified or not. For the evaluation of classical ERP measures, EEG responses were filtered with a low cut-off of 0.1 Hz (12 dB/oct) and a high cut-off of 12 Hz (48 dB/oct) (Ludowig et al., 2008). Event-related potentials were averaged for the interval [−200 ms; 1400 ms] and baseline-corrected with respect to the prestimulus interval [−200 ms; 0 ms]. The peak amplitudes of the rhinal N400 and the hippocampal P600, as well as the mean amplitudes in the intervals [300 ms; 600 ms] (rhinal cortex) and [400 ms; 900 ms] were chosen as ERP measures.

Analysis of power, phase-locking and synchronization changes

EEG responses were filtered in the frequency range from 1 Hz to 49 Hz (1 Hz steps) by continuous wavelet transforms implementing Morlet wavelets with a bandwidth parameter $f_0/\sigma_f=5$, i.e. roughly speaking wavelets of five cycles length (e.g. Lachaux et al., 1999). The complex filtered signals $w_{j,k}$ (j: time point within a trial, k: trial number) hereby result from the time convolution of original signals and the complex wavelet function. In order to avoid edge effects, EEG responses were segmented from −1200 ms to 2400 ms with respect to stimulus onset, and after wavelet-transform 1000 ms at both sides were discarded. Based on the wavelet transformed signals $w_{j,k}$ the phases $\phi_{j,k}$ ($\phi_{j,k}=\arctan(\mathrm{Im}(w_{j,k})/\mathrm{Re}(w_{j,k}))$), the phase differences between rhinal cortex and hippocampus $\Delta\phi_{j,k}=\phi_{j,k}$ (RH)$-\phi_{j,k}$ (HI), and the power values $P_{j,k}$ ($P_{j,k}=\mathrm{Re}(w_{j,k})^2+\mathrm{Im}(w_{j,k})^2$) were extracted for each time point j of each trial k.

The calculation of inter-trial phase-locking and phase synchronization values was done by a procedure suitable for the evaluation of small and unequal trial numbers (e.g. Fell et al., 2004). Distributions of phases (phase-locking) and rhinal–hippocampal phase differences (synchronization) across trials were calculated separately for "remembered" and "forgotten" trials. For this purpose, the phase domain was divided into 8 boxes of 45° covering the range from −180° to +180°. Distribution probabilities X_i were calculated for each box i and each time point j. Phase-locking values PL_j (as well as phase synchronization values) were then evaluated based on a normalized entropy measure: $\mathrm{PL}_j = 1+\sum_{i=1}^{8} X_{i,j} * \log X_{i,j}/\log(8)$. A large phase-locking or synchronization value indicates that phases or phase differences are not uniformly distributed, but exhibit phase accumulations. To allow a finer phase resolution, calculations were iterated for 45 shifts of the boxes about 1°. Finally, the phase-locking and synchronization values resulted from the averages of these iterations. We did not contrast synchronization values against trial-shuffled surrogates (Lachaux et al. 1999), i.e. our synchronization estimates include synchronization caused by stimulus-locked activity within rhinal cortex and hippocampus, which overlaps in the frequency and time domain.

Power, phase-locking and synchronization values were averaged for non-overlapping successive time windows of 100 ms duration from −200 to 1400 ms (16 windows in total). Afterwards, values corresponding to the time windows between −100 and 1400 ms were divided by the prestimulus time window from −200 to −100 ms separately for each subject and each filter frequency. We chose this prestimulus interval as a baseline so that the variation of normalized power, phase-locking and synchronization could be demonstrated for the prestimulus interval between −100 and 0 ms. Power, phase-locking and synchronization values were transformed into a dB scale ($10*\log_{10}$) only for graphical depiction.

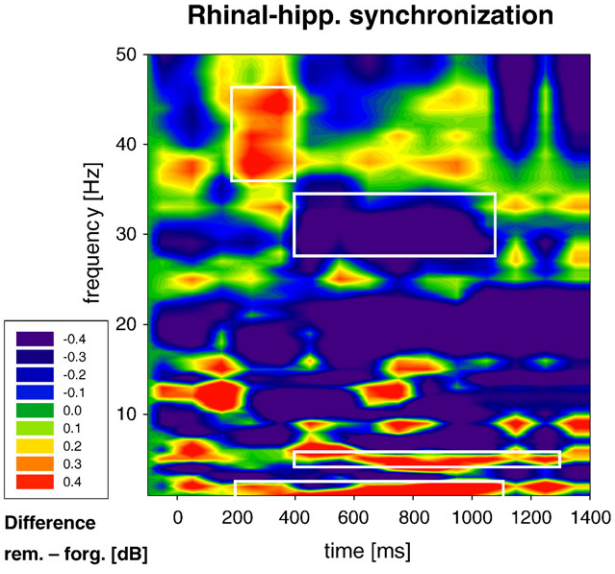

Fig. 3. Difference of changes in rhinal–hippocampal synchronization for remembered versus forgotten words. The plots show color-coded differences of synchronization values, which have been normalized with respect to a prestimulus baseline [−200 to 100 ms] and have been transformed into a dB scale ($10*\log_{10}$). Frequencies between 1 and 49 Hz are represented in y direction while time relative to word presentation is depicted in x direction. EEG measures selected for statistical analysis are indicated by white boxes.

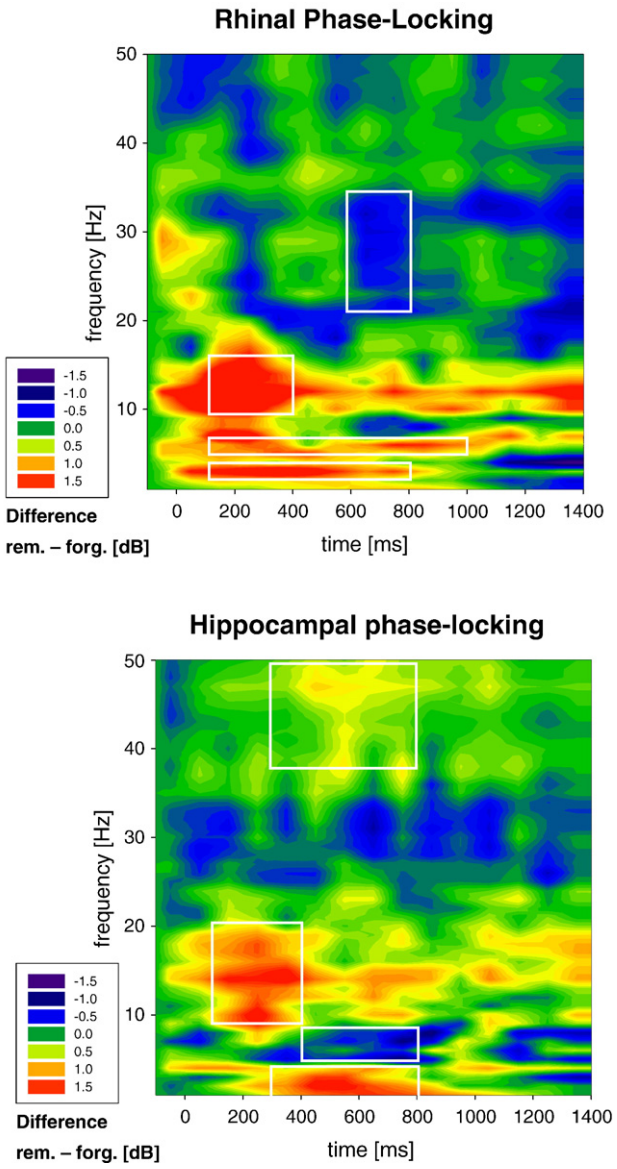

Fig. 4. Difference of phase-locking changes for remembered versus forgotten words (for details see legend of Fig. 2).

Statistical analyses

To evaluate the capability of the different EEG measures to predict successful memory formation paired *t*-tests for the individual measures, MANOVAs for groups of measures and parametric discriminant analyses using pooled covariance matrices were performed (SAS procedure DISCRIM). Into a first discriminant analysis (DISCRIM1) the changes with respect to baseline for subsequently remembered and forgotten words were entered. This discriminant analysis quantifies the ability of a certain measure, to identify the class (remembered, forgotten) to which an average response belongs, when only the response for this class (and not the response for the other class) is given. Furthermore, a stepwise discriminant analysis with a significance level of $p=0.05$ for entering and staying in the model was performed. For a second discriminant analysis (DISCRIM2) the changes were normalized to the average change across the classes (remembered, forgotten). This discriminant analysis quantifies the capability to identify responses corresponding to later remembered or forgotten words, when the responses for both classes are given.

Results

Behavioral data

On average, 66.7 ± 21.3% of presented words were later successfully remembered. Performance did not differ between patients with left and right focal hemisphere ($t_{30}=0.518$, $p=0.61$) or between male and female patients ($t_{30}=0.875$, $p=0.39$). Reaction times did also not differ between subsequently remembered and forgotten words (remembered: 878 ± 161 ms; forgotten: 882 ± 232 ms, paired *t*-test: $t_{30}=0.175$, $p=0.86$).

Qualitative EEG effects

Fig. 2 shows the ERP responses for later remembered and forgotten words. In accordance with previous data, the rhinal N400 and the hippocampal P600 component are increased for later remembered compared to forgotten words. Figs. 3–5 depict the differences in synchronization, phase-locking and power between the responses to later remembered versus forgotten words. The synchronization, phase-locking and power changes are displayed separately for remembered and forgotten words in Figs. 6 and 7. Consistent with

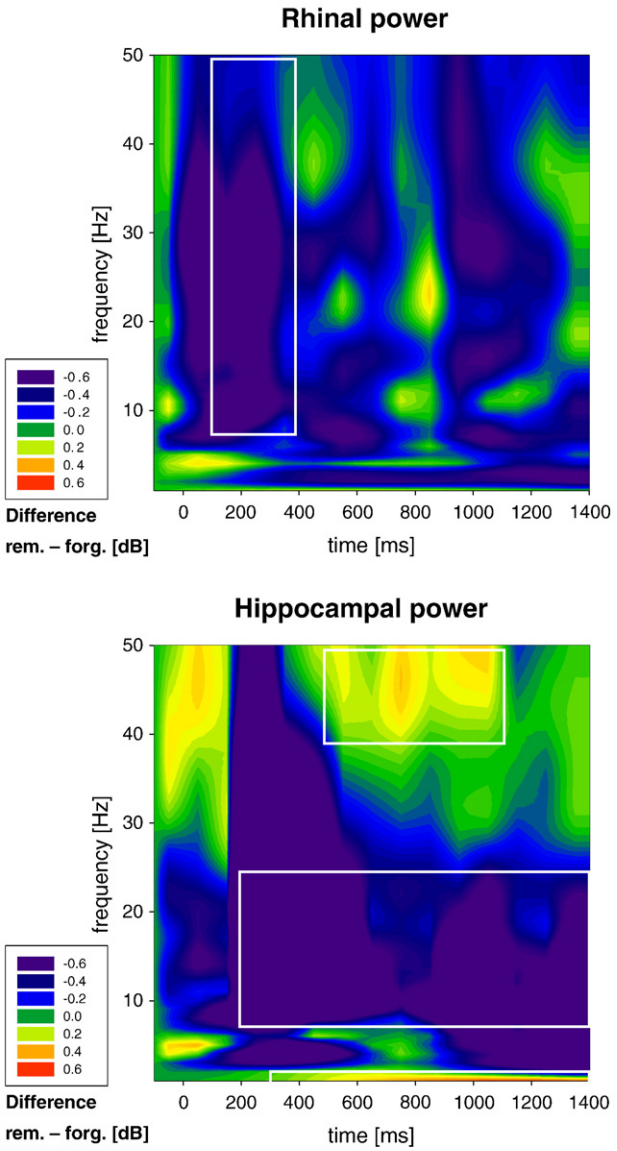

Fig. 5. Difference of power changes for remembered versus forgotten words (for details see legend of Fig. 2).

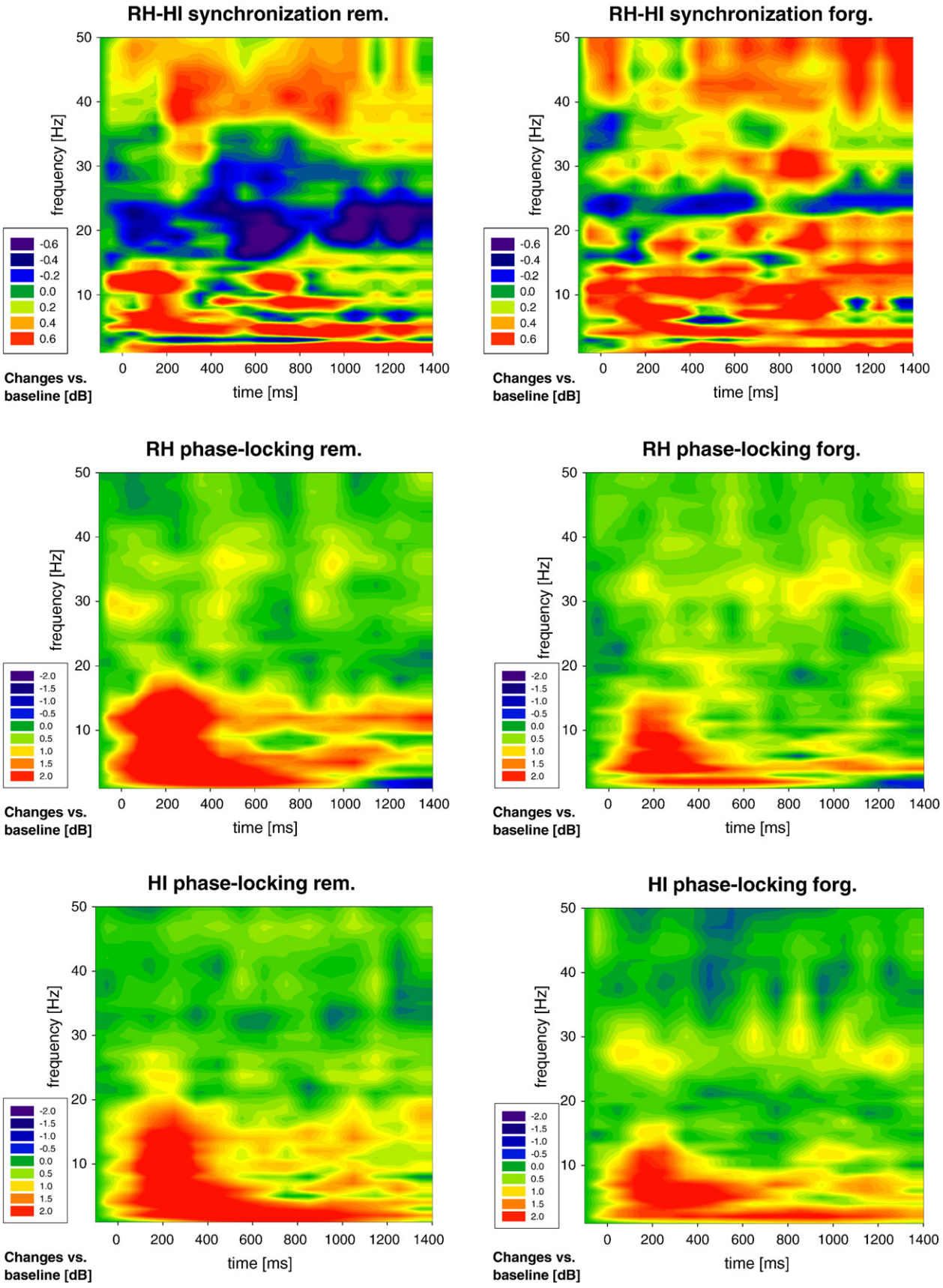

Fig. 6. Changes of rhinal–hippocampal synchronization, as well as rhinal and hippocampal phase-locking separately for remembered (left) and forgotten (right) words (for details see legend of Fig. 2).

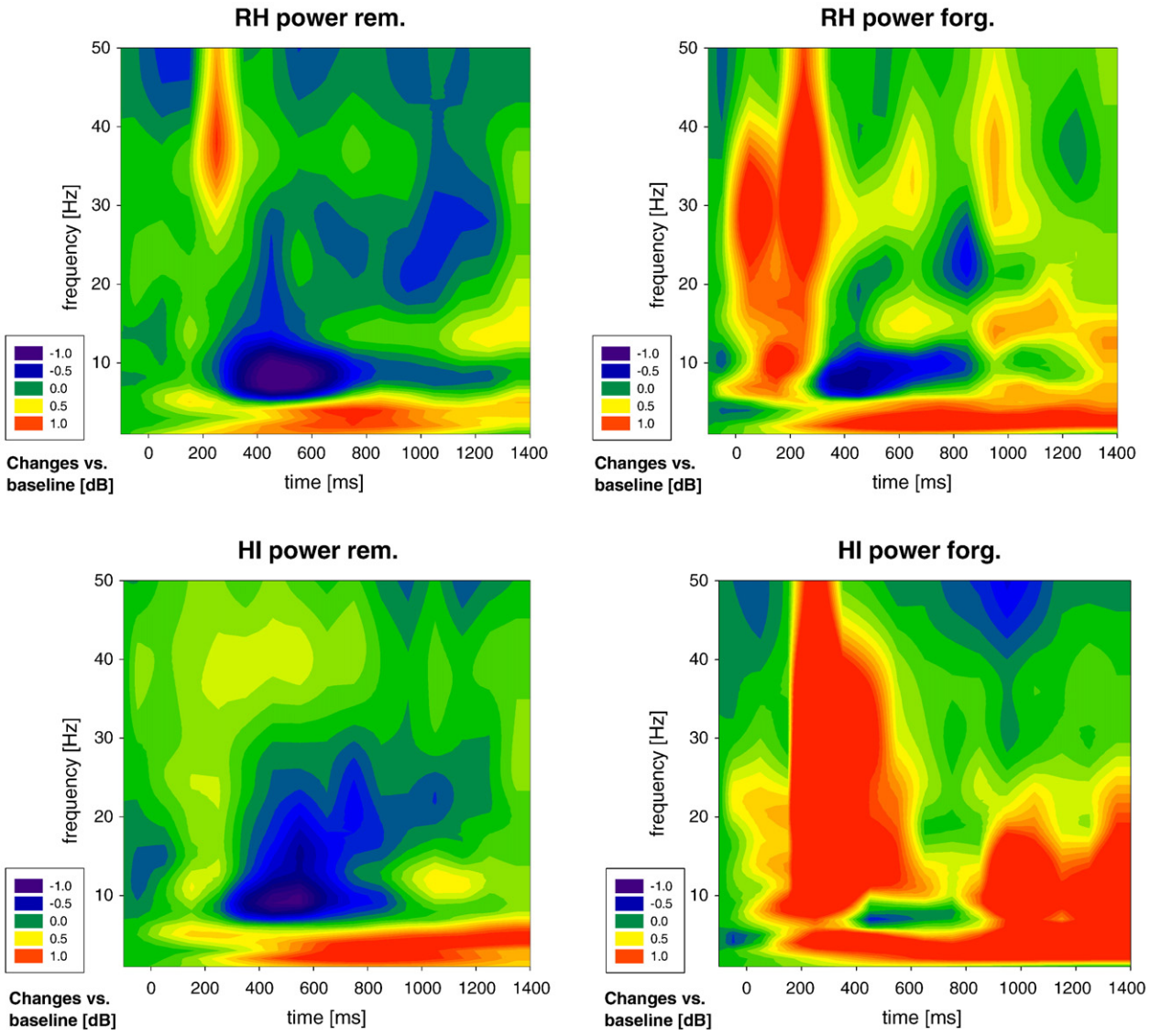

Fig. 7. Changes of rhinal and hippocampal power separately for remembered (left) and forgotten (right) words (for details see legend of Fig. 2).

our prior findings, we observed an early increase of rhinal–hippocampal gamma synchronization and a later decrease (Fell et al., 2001), as well as a synchronization increase in the delta and theta range (Fell et al., 2003). These effects are in the order of ±0.4 dB (equivalent to around ±10%). The most pronounced subsequent memory effects in the range of ±1.5 dB (equivalent to around ±40%), however, were observed for rhinal and hippocampal phase-locking. In accordance to prior data related to the continuous recognition task (Mormann et al., 2005), rhinal phase-locking mainly occurred in the delta, theta and alpha/beta range. A phase-locking decrease was observed for the lower gamma range. Hippocampal phase-locking was detected in the delta, alpha/beta and gamma range. In contrast to the rhinal recordings, a decrease of hippocampal phase-locking occurred in the theta range. Finally, memory-related rhinal and hippocampal power changes were observed in the order of ±0.6 dB (equivalent to around ±15%). Within rhinal cortex, an early broad-band decrease of power in the alpha/beta/gamma range was detected. Within the hippocampus, an increase of delta power, as well as an increase of upper gamma power and a decrease of power mainly in the alpha/beta range was found. The latter effects are in accordance with the findings of Sederberg et al. (2007).

Selection of the EEG measures

Based on the apriori hypotheses and the observed subsequent memory effects five different groups of measures were composed: classical ERP components, rhinal–hippocampal synchronization, rhinal phase-locking, hippocampal phase-locking, rhinal and hippocampal power. For each group four measures were selected, which are listed in Table 1 (see also Figs. 2–5). Besides measures based on apriori hypotheses (e.g. gamma and theta synchronization), those with the largest remembered versus forgotten differences were chosen under the condition that they had an extension of at least 10 time (100 ms)*frequency (1 Hz) voxels.

Statistical evaluation of subsequent memory effects

When comparing baseline related changes for remembered versus forgotten responses by paired two-tailed *t*-tests (see Table 2), nine of the twenty EEG measures yielded a significant effect ($p<0.05$). The clearly largest effects were reached by three phase-locking measures: rhinal alpha/beta phase-locking (difference between average changes with respect to baseline for remembered and forgotten

Table 1
Overview of EEG measures selected for statistical analysis

	Time range [ms]	Frequency range [Hz]
ERP components		
Rhinal N4	Peak	–
Hippocampal P6	Peak	–
Rhinal N4 area	300–600	–
Hippocampal P6 area	400–900	–
Synchronization		
Delta ↑	200–1100	1–2
Theta ↑	400–1300	5
Gamma ↓	400–1100	28–34
Gamma ↑	200–400	37–46
Phase-locking (RH)		
Delta ↑	100–800	2–3
Theta ↑	100–1000	5–6
AlphaBeta ↑	100–400	10–16
Gamma ↓	600–800	21–34
Phase-locking (HI)		
Delta ↑	300–800	1–4
Theta ↓	400–800	5–8
AlphaBeta ↑	100–400	9–20
Gamma ↑	300–800	38–49
Power		
RH: AlphaBetaGamma ↓	100–400	8–49
HI: Delta ↑	300–1400	1
HI: AlphaBeta ↓	200–1400	8–24
HI: Gamma ↑	500–1100	39–49

words (rem.–forg.): 70.7%, $p<0.0001$), as well as hippocampal delta (rem.–forg.: 39.6%, $p<0.001$) and alpha/beta (rem.–forg.: 36.6%, $p=0.001$) phase-locking. Indeed, a stepwise discriminant analysis included into the best model two of those measures (rhinal alpha/beta and hippocampal delta phase-locking) plus hippocampal gamma

Table 2
Average changes with respect to baseline for the selected measures

	Remembered		Forgotten		Paired *t*-test
	Mean	SEM	Mean	SEM	*p*-Value
ERP components [μV]					
Rhinal N4	−53.21	6.38	−49.44	6.19	n.s. (0.103)
Hippocampal P6	54.99	9.06	50.20	8.27	n.s. (0.267)
Rhinal N4 mean	−36.59	4.63	−29.52	4.63	0.038
Hippocampal P6 mean	25.60	6.62	16.63	5.39	0.048
Synchronization [%]					
Delta ↑	35.10	9.94	20.79	7.45	n.s. (0.153)
Theta ↑	19.17	9.87	9.31	9.09	n.s. (0.409)
Gamma ↓	−1.64	3.98	9.04	4.73	0.035
Gamma ↑	13.96	4.58	4.85	2.75	n.s. (0.090)
RH phase-locking [%]					
Delta ↑	93.48	16.72	45.30	12.53	0.014
Theta ↑	77.89	13.61	40.42	9.64	0.026
AlphaBeta ↑	103.53	15.38	32.80	8.14	<0.0001
Gamma ↓	1.49	4.08	13.38	3.65	0.028
HI phase-locking [%]					
Delta ↑	78.64	9.99	39.07	8.50	<0.001
Theta ↓	29.38	7.76	42.21	10.78	n.s. (0.361)
AlphaBeta ↑	59.91	9.56	23.29	6.23	0.001
Gamma ↑	6.66	4.46	−2.10	3.13	n.s. (0.107)
Power [%]					
RH: AlphaBetaGamma ↓	4.34	1.40	19.66	10.69	n.s. (0.160)
HI: Delta ↑	14.79	3.83	4.78	4.86	n.s. (0.162)
HI: AlphaBeta ↓	−1.97	2.56	34.26	18.82	n.s. (0.065)
HI: Gamma ↑	3.22	2.23	−1.27	2.23	n.s. (0.104)

p-Values indicate significance levels for paired two-tailed *t*-tests comparing changes corresponding to subsequently remembered and forgotten responses.

Table 3
Statistical separation of EEG responses corresponding to subsequently remembered and forgotten words

	MANOVA $F_{4,49}$	*p*-Value	DISCRIM1 error rate %			DISCRIM2 error rate %
			rem.	mean	forg.	
ERP components	0.980	0.427	33.3	40.7	48.2	22.2
Synchronization	2.326	0.069	37.0	35.2	33.3	25.9
Phase-locking (RH)	6.640	0.0002	29.6	22.2	14.8	7.4
Phase-locking (HI)	6.489	0.0003	25.9	22.2	18.5	18.5
Power	2.070	0.099	29.6	35.2	40.7	29.6
Best four	10.607	<0.00001	18.5	18.5	18.5	3.7

Results of MANOVAs and discriminant analyses for the different groups of EEG measures are shown.

phase-locking (rem.–forg.: 8.8%, $p=0.107$) and the rhinal–hippocampal gamma synchronization increase (rem.–forg.: 9.1%, $p=0.090$), in the following order: 1) ↑ Rhinal alpha/beta phase-locking; 2) ↑ Rhinal–hippocampal gamma synchronization; 3) ↑ Hippocampal delta phase-locking; 4) ↑ Hippocampal gamma phase-locking. Also MANOVAs for the different groups of measures (see Table 3) produced the by far most significant effects for phase-locking within rhinal cortex ($p=0.0002$) and within the hippocampus ($p=0.0003$). However, the best model selected by stepwise discriminant analysis yielded a superior MANOVA effect of $p<10^{-5}$. The only group for which no significant effect or trend was detected are the classical ERP measures.

The discriminant analysis without normalization across classes (DISCRIM1; see Materials and methods) yielded error rates of 22.2% for the prediction of subsequent memory based on the rhinal or the hippocampal phase-locking measures (see Table 3). For the best model the prediction error amounted to 18.5%. The highest error rate (40.7%) was observed for the classical ERP measures. For rhinal–hippocampal synchronization and the phase-locking measures, prediction of later forgetting was better then prediction of later remembering (e.g. error rate of 14.8% versus 29.6% for rhinal phase-locking). For the classical ERP measures and power changes, the opposite was the case. Finally, the discriminant analysis with normalization across classes (DISCRIM2) revealed considerably lower error rates: 22.2% for the classical

Table 4
Statistical separation of EEG responses corresponding to subsequently remembered and forgotten words: discriminant analyses for those individual EEG measures, which showed a significant remembered/forgotten effect or trend ($p<0.1$) for the paired *t*-tests, as well as for the variable "rhinal alpha/beta phase-locking*hippocampal alpha/beta phase-locking"

	DISCRIM1 error rate %			DISCRIM2 error rate %
	rem.	mean	forg.	
ERP components				
Rhinal N4 mean	48.2	48.2	48.2	25.9
Hippocampal P6 mean	51.9	44.4	37.0	40.7
Synchronization				
Gamma ↓	37.0	38.9	40.7	25.9
Gamma ↑	44.4	38.9	33.3	40.7
RH phase-locking				
Delta ↑	51.9	42.6	33.3	29.6
Theta ↑	40.7	37.0	33.3	40.7
AlphaBeta ↑	44.4	31.5	18.5	14.8
Gamma ↓	40.7	38.9	37.0	37.0
HI Phase-locking				
Delta ↑	40.7	35.2	29.6	14.8
AlphaBeta ↑	37.0	31.5	26.0	22.2
Power				
HI: AlphaBeta ↓	11.1	37.0	63.0	14.8
RH phase-locking AlphaBeta× HI phase-locking AlphaBeta	40.7	24.1	7.4	11.1

ERP measures, 7.4% for rhinal-phase-locking and 3.7% for the best model. This means that knowledge of responses for both classes significantly improves the prediction of subsequent memory.

Individual discriminant analyses for those EEG measures, which showed a significant remembered/forgotten effect or trend ($p<0.1$) for the paired *t*-tests, are depicted in Table 4. Discriminant analysis without normalization across classes yielded lowest error rates (31.5%) for rhinal and hippocampal alpha/beta phase-locking. Discriminant analysis with normalization across classes revealed lowest error rates (14.8%) for rhinal alpha/beta and hippocampal delta phase-locking, as well as for hippocampal alpha/beta power reduction. We furthermore analyzed, whether concurrent rhinal and hippocampal alpha/beta phase-locking is predictive for memory formation by entering the product between both measures as discriminant variable (see Table 4). Indeed, this measure yielded even lower error rates than rhinal phase-locking alone (24.1% and 11.1%, respectively).

Discussion

In the present study we evaluated the capability of several groups of mediotemporal EEG measures to differentiate between subsequently remembered and forgotten words: amplitudes of ERP components, rhinal–hippocampal phase synchronization, as well as inter-trial phase-locking and power changes. In accordance to prior investigations, we observed a memory-related increase of the rhinal N400 component and the later hippocampal positivity (Fernández et al., 1999, 2002), an enhanced rhinal–hippocampal phase synchronization in the gamma and the low frequency range (Fell et al., 2001; 2003), as well as a hippocampal power increase in the upper gamma range and a power decrease in the alpha and beta range (Sederberg et al., 2007).

The best predictors of subsequent memory, however, were the phase-locking characteristics, most notably rhinal phase-locking in the alpha/beta range. This finding represents an important advance over previous reports. Fig. 8 illustrates the rhinal alpha/beta phase-locking effect for one patient. For trials corresponding to remembered (above) compared to forgotten words (below) a stronger alignment of peaks and troughs in the vertical direction is observable. Generally, the memory-related phase-locking effects seem to exhibit a very early onset already within 100 ms after word presentation. Of course, one has to account for the temporal resolution of the wavelet-transform, which may be estimated as the half width at half maximum of the Gaussian envelope of the Morlet wavelet (e.g. Baudin et al., 1994), yielding, for instance, 94 ms for 10 Hz, or 67 ms for 14 Hz. Still, this means that the rhinal phase-locking effect may already start around 100 ms and reaches its maximum in the time window between 100 and 300 ms after stimulus onset. This phase-locking increase reflects the precise onset of an alpha/beta oscillation contributing to the rising edge of the rhinal N400 component. The early timing suggests that mediotemporal phase-locking may be initiated by an attentional top-down process mediated directly by the thalamus (LaBerge, 1997). This process may prepare for the arrival of detailed stimulus information from higher-order visual areas, which is not to be expected before 200 ms after word presentation (e.g. Nobre et al., 1994). Our findings are reminiscent of the reported reset of human neocortical oscillations in the theta/alpha/beta range during a working memory task (Rizzuto et al., 2003).

It may be speculated that the concurrence of rhinal and hippocampal alpha/beta phase-locking has a significant impact on neurons receiving information from both the rhinal cortex and the hippocampus, for instance neurons in the subiculum (e.g. Behr et al., 1998). This effect may be qualitatively similar to the impact of rhinal–hippocampal synchronization. Actually, there is a circumscribed memory-related increase of rhinal–hippocampal synchronization between 10 and 14 Hz and 100 and 200 ms (Fig. 3), which may correspond to the concurrent rhinal and hippocampal alpha/beta phase-locking. Moreover, we observed the lowest discrimination error rates for the variable resulting from the product of rhinal and hippocampal phase-locking. For this variable, discrimination accuracy was even better than for rhinal phase-locking alone. This finding yields strong evidence for the idea that concurrent rhinal and hippocampal alpha-beta phase-locking is crucial for successful memory formation.

Interestingly, the rhinal phase-locking increase in the alpha/beta range is accompanied by a broad-band decrease of rhinal power in the alpha, beta and gamma range. This power decrease, which similarly occurs within the hippocampus, may be related to a shut down of ongoing neural activity in order to prepare for incoming sensory information. Moreover, our data suggest that the phase-locking increase results from a phase-reset of ongoing oscillations and not from additive stimulus-locked activity, although the evidence is not conclusive (e.g. Hanslmayr et al., 2007). As a consequence, the subsequent memory effects for the rhinal N400 peak and the mean N400 amplitude are rather small, in spite of the strong and concentrated phase-locking effect (which, in principle, should particularly boost the N400 peak amplitude). This result underlines the need for a separation of phase-locking and power changes, because both aspects contribute to cognitive ERPs and may dissociate between conditions (e.g. Fell, 2007).

Actually, the ERP and phase synchronization effects observed in the present investigation are smaller than those found in previous studies (e.g. a memory-related gamma synchronization increase of up to 14% compared to up to 30% in Fell et al., 2001). There may be two major reasons for this outcome: First of all, encoding-related activations in item recognition paradigms are typically less pronounced than activations observed in free recall paradigms (e.g. Staresina and Davachi, 2006). Second, the task of encoding new words is overlaid with the task of recognizing previously presented words in the continuous recognition paradigm, which may have partly clouded the encoding-related effects. Furthermore, subsequent memory effects in the continuous word recognition paradigm have been shown to vary considerably along the longitudinal axis of the hippocampus (Ludowig et al., 2008). For the present study, we selected electrode contacts based on the largest memory-related ERP components across conditions (remembered, forgotten), in order to minimize the bias towards a certain group of measures.

The best model as selected by a stepwise discriminant analysis, besides three phase-locking measures (rhinal alpha/beta and hippocampal delta and gamma phase-locking), included the rhinal–hippocampal synchronization increase in the gamma range. This means that the four measures contain independent information, which maximizes predictive power. In particular, hippocampal phase-locking in the gamma range and rhinal–hippocampal gamma synchronization appear to represent EEG characteristics that are not redundant. Indeed, Pearson's correlation between both measures is rather small ($r=-0.11$; n.s.). On the other hand, there is a significant correlation between rhinal and hippocampal alpha/beta phase-locking ($r=0.36$; $p<0.05$). Consequently, hippocampal alpha/beta phase-locking was not included into the best model, in spite of its highly significant capability to distinguish between responses corresponding to later remembered and forgotten words.

While discriminant analyses without normalization across classes yielded error rates around 20% for the prediction of subsequent memory based on the phase-locking measures or based on the best model, prediction errors of only 7.4% for rhinal phase-locking and of 3.7% for the best model were reached with discriminant analyses including normalization across classes. This result is probably caused by the fact that the average level of the phase-locking responses for both, later remembered and forgotten words varies considerably across subjects. For instance, for rhinal alpha/beta phase-locking the standard errors corresponding to remembered (15.4%) and forgotten (8.1%) items are larger than the standard errors for the difference

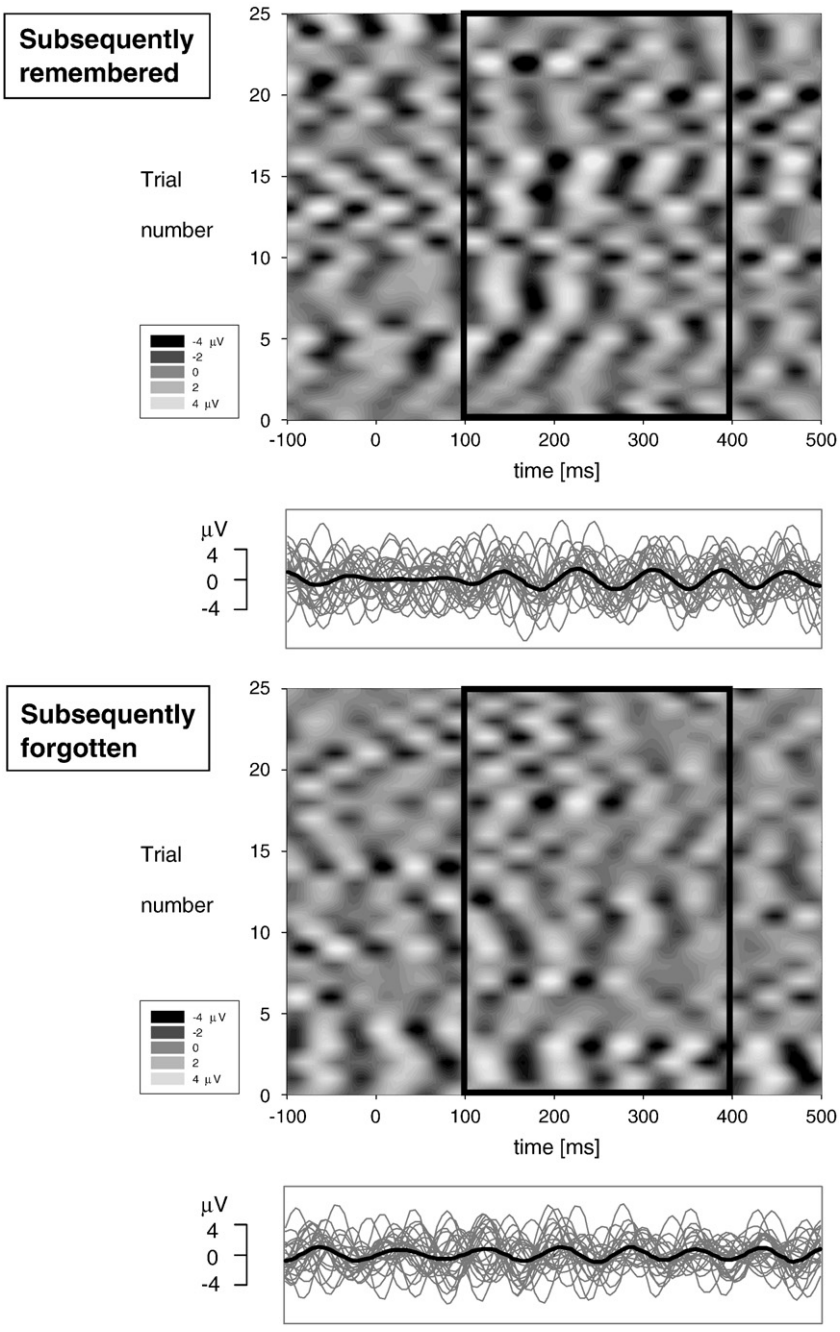

Fig. 8. Illustration of rhinal alpha/beta phase-locking for one patient. Rhinal recordings were filtered in the frequency range between 12 and 14 Hz (Butterworth Filter, 48 dB/octave). On the *y*-axis the first 25 trials corresponding to later remembered (above) and later forgotten words (below) are depicted. Time with respect to word presentation is depicted on the *x*-axis. EEG voltage is coded by a gray scale (black: max. negative voltage; white: max. positive voltage). Alpha/beta phase-locking is reflected by the alignment of peaks and throughs in the vertical direction. Below the gray-scale plots the same trials are depicted as superimposed waveforms (gray) and averages (black).

between both classes (6.8%). Accounting for this variability by normalizing across classes, which practically implies a prediction based on knowledge of responses for both, later remembered and forgotten words, results in a much higher prediction accuracy. Interestingly, prediction of later forgetting is better than prediction of remembering for the phase-locking and synchronization measures, i.e. it seems easier to determine when memory formation fails than when it succeeds.

It is yet an open question how the increased mediotemporal phase-locking may be functionally interpreted. Generally, an enhancement of phase-locking indicates that the timing of stimulus processing related to oscillations within a certain frequency band exhibits less inter-trial variability. It has been suggested that slow EEG waves provide a threshold controlling the excitability of cortical networks (Elbert and Rockstroh, 1987; Schupp et al., 1994). Indeed, it has been shown that, for instance, the phase of theta oscillations modulates the amplitude of gamma activity (e.g. Chrobak and Buzsáki, 1998; Canolty et al., 2006; Mormann et al., 2005), which is probably closely related to the strength of neural firing (e.g. Mukamel et al., 2005). Such a mechanism may contribute to the so-called hippocampal phase coding, i.e. to the coding of neural memory representations by the phase of a low frequency oscillation (e.g. Jensen and Lisman 2005). In this sense, the increased mediotemporal phase-locking may support a phase representation of to be memorized material.

More generally, precise timing of the phase of EEG responses may reflect inhibition or facilitation of neural firing occurring exactly at the

right time point within the required sequence of neural processing. It is, for instance, conceivable that the early mediotemporal phase-reset in the alpha-beta range triggers rhinal–hippocampal phase synchronization and prepares for the later increase of hippocampal gamma activity. Our findings furthermore underline the role of alpha-phase dynamics in memory processes, which has previously been shown for surface EEG and MEG data (e.g. Herrmann et al., 2004; Klimesch et al., 2004; Palva and Palva 2007). To summarize, our data demonstrate that memory encoding is closely associated with early phase adjustments within the MTL.

Acknowledgments

The authors would like to thank Christian Bien for the support with the clinical management of the patients and Horst Urbach for providing the magnetic resonance images. We furthermore thank two anonymous referees for their helpful comments and suggestions. This research was supported by the Deutsche Forschungsgemeinschaft (Transregional Collaborative Research Centre SFB/TR 3, project A3), as well as by the Volkswagen Foundation (grant number: I/79878).

References

Baudin, F., Gabriel, A., Gibert, D., 1994. Time/frequency analysis of solar p-modes. Astronomy and Astrophysics 285, 29–32.
Behr, J., Gloveli, T., Heinemann, U., 1998. The perforant path projection from the medial entorhinal cortex layer III to the subiculum in the rat combined hippocampal–entorhinal slice. Eur. J. Neurosci. 10, 1011–1018.
Canolty, R.T., Edwards, E., Dalal, S.S., Soltani, M., Nagarajan, S.S., Kirsch, H.E., Berger, M.S., Barbaro, N.M., Knight, R.T., 2006. High gamma power is phase-locked to theta oscillations in human neocortex. Science 313, 1626–1628.
Chrobak, J.J., Buzsáki, G., 1998. Gamma oscillations in the entorhinal cortex of the freely behaving rat. J. Neurosci. 18, 388–398.
Duvernoy, H.M., 1988. The human hippocampus. An atlas of applied anatomy. J. F. Bergmann Verlag, München, pp. 25–43.
Elbert, T., Rockstroh, B., 1987. Threshold regulation—a key to the understanding of the combined dynamics of EEG and event-related potentials. J. Psychophysiol. 4, 317–333.
Eichenbaum, H., 2000. A cortical–hippocampal system for declarative memory. Nat. Rev. Neurosci. 1, 41–50.
Fell, J., 2007. Cognitive neurophysiology: beyond averaging. Neuroimage 37, 1069–1072.
Fell, J., Klaver, P., Lehnertz, K., Grunwald, T., Schaller, C., Elger, C.E., Fernández, G., 2001. Human memory formation is accompanied by rhinal–hippocampal coupling and decoupling. Nat. Neurosci. 4, 1259–1264.
Fell, J., Klaver, P., Elfadil, H., Schaller, C., Elger, C.E., Fernández, G., 2003. Rhinal–hippocampal theta coherence during declarative memory formation: interaction with gamma-synchronization? Eur. J. Neurosci. 17, 1082–1088.
Fell, J., Dietl, T., Grunwald, T., Kurthen, M., Klaver, P., Trautner, P., Schaller, C., Elger, C.E., Fernández, G., 2004. Neural bases of cognitive ERPs: more than phase reset. J. Cogn. Neurosci. 16, 1595–1604.
Fernández, G., Effern, A., Grunwald, T., Pezer, N., Lehnertz, K., Dümpelmann, M., Van Roost, D., Elger, C.E., 1999. Real-time tracking of memory formation in the human rhinal cortex and hippocampus. Science 285, 1582–1585.
Fernández, G., Klaver, P., Fell, J., Grunwald, T., Elger, C.E., 2002. Human declarative memory formation: segregating rhinal and hippocampal contributions. Hippocampus 12, 514–519.
Grunwald, T., Elger, C.E., Lehnertz, K., Van Roost, D., Heinze, H.J., 1995. Alterations of intrahippocampal cognitive potentials in temporal lobe epilepsy. Electroencephalogr. Clin. Neurophysiol. 95, 53–62.
Grunwald, T., Beck, H., Lehnertz, K., Blümcke, I., Pezer, N., Kurthen, M., Fernández, G., Van Roost, D., Heinze, H.J., Kutas, M., Elger, C.E., 1999. Evidence relating human verbal memory to hippocampal *N*-methyl-D-asparate receptors. Proc. Natl. Acad. Sci. U. S. A. 96, 12085–12089.
Hanslmayr, S., Klimesch, W., Sauseng, P., Gruber, W., Doppelmayr, M., Freunberger, R., Pecherstorfer, T., Birbaumer, N., 2007. Alpha phase reset contributes to the generation of ERPs. Cereb. Cortex 17, 1–8.
Helmstaedter, C., Fritz, N.E., González Pérez, P.A., Elger, C.E., Weber, B., 2006. Shift-back of right to left hemisphere language dominance after control of epileptic seizures: evidence for epilepsy driven functional cerebral organization. Epilepsy Res. 70, 257–262.
Herrmann, C.S., Senkowski, D., Röttger, S., 2004. Phase-locking and amplitude modulations of EEG alpha: two measures reflect different cognitive processes in a working memory task. Exp. Psychol. 51, 311–318.
Jensen, O., Lisman, J.E., 2005. Hippocampal sequence-encoding driven by a cortical multi-item working memory buffer. Trends Neurosci. 28, 67–72.
Klimesch, W., Schack, B., Schabus, M., Doppelmayr, M., Gruber, W., Sauseng, P., 2004. Phase-locked alpha and theta oscillations generate the P1–N1 complex and are related to memory performance. Cogn. Brain Res. 19, 302–316.
LaBerge, D., 1997. Attention, awareness, and the triangular circuit. Conscious Cogn. 6, 149–181.
Lachaux, J.P., Rodriguez, E., Martinerie, J., Varela, F.J., 1999. Measuring phase synchrony in brain signals. Hum. Brain Mapp. 8, 194–208.
Ludowig, E., Trautner, P., Kurthen, M., Schaller, C., Bien, C.G., Elger, C.E., Rosburg, T., 2008. Intracranially recorded memory-related potentials reveal higher posterior than anterior hippocampal involvement in verbal encoding and retrieval. J. Cogn. Neurosci. Jan 17 [Epub ahead of print].
Makeig, S., Debener, S., Onton, J., Delorme, A., 2004. Mining event-related brain dynamics. Trends Cogn. Sci. 8, 204–210.
Mazaheri, A., Jensen, O., 2006. Posterior alpha activity is not phase-reset by visual stimuli. Proc. Natl. Acad. Sci. U. S. A. 103, 2948–2952.
Mormann, F., Fell, J., Axmacher, N., Weber, B., Lehnertz, K., Elger, C.E., Fernández, G., 2005. Phase/amplitude reset and theta–gamma interaction in the human mediotemporal lobe during a continuous word recognition memory task. Hippocampus 15, 890–900.
Mukamel, R., Gelbard, H., Arieli, A., Hasson, U., Fried, I., Malach, R., 2005. Coupling between neuronal firing, field potentials, and fMRI in human auditory cortex. Science 309, 951–954.
Nobre, A.C., Allison, T., McCarthy, G., 1994. Word recognition in the human inferior temporal lobe. Nature 372, 260–263.
Paller, K.A., Mc Carthy, G., Roessler, E., Allison, T., Wood, C.C., 1992. Potentials evoked in human and monkey mediotemporal lobe during auditory and visual oddball paradigms. Electroencephalogr. Clin. Neurophysiol. 84, 269–279.
Palva, S., Palva, J.M., 2007. New vistas for alpha-frequency band oscillations. Trends Neurosci. 30, 150–158.
Puce, A., Kalnins, R.M., Berkovic, S.F., Donnan, G.A., Bladin, P.F., 1989. Limbic P3 potentials, seizure localization, and surgical pathology in temporal lobe epilepsy. Ann. Neurol. 26, 377–385.
Rizzuto, D.S., Madsen, J.R., Bromfield, E.B., Schulze-Bonhage, A., Seelig, D., Aschenbrenner-Scheibe, R., Kahana, M.J., 2003. Reset of human neocortical oscillations during a working memory task. Proc. Natl. Acad. Sci. U. S. A. 100, 7931–7936.
Schupp, H.T., Lutzenberger, W., Rau, H., Birbaumer, N., 1994. Positive shifts of event-related potentials: a state of cortical disfacilitation as reflected by the startle reflex probe. Electroencephalogr. Clin. Neurophysiol. 90, 135–144.
Sederberg, P.B., Schulze-Bonhage, A., Madsen, J.R., Bromfield, E.B., McCarthy, D.C., Brandt, A., Tully, M.S., Kahana, M.J., 2007. Hippocampal and neocortical gamma oscillations predict memory formation in humans. Cereb. Cortex 17, 1190–1196.
Squire, L.R., Stark, C.E., Clark, R.E., 2004. The mediotemporal lobe. Annu. Rev. Neurosci. 2004; 27, 279–306.
Staresina, B.P., Davachi, L., 2006. Differential encoding mechanisms for subsequent associative recognition and free recall. J. Neurosci. 26, 9162–9172.
Van Roost, D., Solymosi, L., Schramm, J., Van Oosterwyck, B., Elger, C.E., 1998. Depth electrode implantation in the length axis of the hippocampus for the presurgical evaluation of mediotemporal lobe epilepsy: a computed tomography-based stereotactic insertion technique and its accuracy. Neurosurgery 43, 819–826.